American Mineralogist, Volume 93, pages 81–87, 2008

Menezesite, the first natural heteropolyniobate, from Cajati, São Paulo, Brazil: Description and crystal structure

Daniel Atencio,[1,*] José M.V. Coutinho,[1] Antonio C. Doriguetto,[2] Yvonne P. Mascarenhas,[3] Javier Ellena,[2] and Viviane C. Ferrari[1]

[1]Instituto de Geociências, Universidade de São Paulo, Rua do Lago, 562, 05508-080, São Paulo, SP, Brazil
[2]Departamento de Ciências Exatas, Universidade Federal de Alfenas, Rua Gabriel Monteiro da Silva, 714, 37130-000, Alfenas, MG, Brazil
[3]Instituto de Física de São Carlos, Universidade de São Paulo, Caixa Postal 369, 13560-970, São Carlos, SP, Brazil

Abstract

Menezesite, ideally $Ba_2MgZr_4(BaNb_{12}O_{42})\cdot 12H_2O$, occurs as a vug mineral in the contact zone between dolomite carbonatite and "jacupirangite" (=a pyroxenite) at the Jacupiranga mine, in Cajati county, São Paulo state, Brazil, associated with dolomite, calcite, magnetite, clinohumite, phlogopite, ancylite-(Ce), strontianite, pyrite, and tochilinite. This is also the type locality for quintinite-2*H*. The mineral forms rhombododecahedra up to 1 mm, isolated or in aggregates. Menezesite is transparent and displays a vitreous luster; it is reddish brown with a white streak. It is non-fluorescent. Mohs hardness is about 4. Calculated density derived from the empirical formula is 4.181 g/cm^3. It is isotropic, $n_{meas} > 1.93(1)$ (white light); $n_{calc} = 2.034$. Menezesite exhibits weak anomalous birefringence. The empirical formula is $(Ba_{1.47}K_{0.53}Ca_{0.31}Ce_{0.17}Nd_{0.10}Na_{0.06}La_{0.02})_{\Sigma 2.66}(Mg_{0.94}Mn_{0.23}Fe_{0.23}Al_{0.03})_{\Sigma 1.43}(Zr_{2.75}Ti_{0.96}Th_{0.29})_{\Sigma 4.00}[(Ba_{0.72}Th_{0.26}U_{0.02})_{\Sigma 1.00}(Nb_{9.23}Ti_{2.29}Ta_{0.36}Si_{0.12})_{\Sigma 12.00}O_{42}]\cdot 12H_2O$. The mineral is cubic, space group $Im\overline{3}$ (204), $a = 13.017(1)$ Å, $V = 2206(1)$ Å^3, $Z = 2$. Menezesite is isostructural with the synthetic compound $Mg_7[MgW_{12}O_{42}](OH)_4\cdot 8H_2O$. The mineral was named in honor of Luiz Alberto Dias Menezes Filho (born 1950), mining engineer, mineral collector and merchant. Both the description and the name were approved by the CNMMN-IMA (Nomenclature Proposal 2005-023). Menezesite is the first natural heteropolyniobate. Heteropolyanions have been employed in a range of applications that include virus-binding inorganic drugs (including the AIDs virus), homogeneous and heterogeneous catalysts, electro-optic and electrochromic materials, metal and protein binding, and as building blocks for nanostructuring of materials.

Keywords: Menezesite, new mineral, polyoxometalates, heteropolyniobate, heteropolyanions, crystal structure, chemical composition, Jacupiranga mine, Cajati, Brazil

Introduction

Menezesite is the first natural heteropolyniobate. Polyoxometalates are a large and rapidly growing class of compounds. Heteropolyoxoanions are negatively charged clusters of corner- and edge-sharing early transition-metal MO_6 octahedra (*M* usually Mo, W, V, Nb, or Ta) and heteroatom located in the interior of the cluster. Over half of the elements in the periodic table are known to function as heteroatoms in heteropoly compounds. The "heteropolyniobates" obtained by Dale and Pope (1967), Dale et al. (1969), and Flynn and Stucky (1969a, 1969b) are not heteropolyoxoniobates sensu stricto, because the ligands do not form a cage about the heteroatom. The first heteropolyoxometalate, $(NH_4)_3[PMo_{12}O_{40}]$, was obtained by Berzelius (1826) as a yellow crystalline precipitate. The formation of this precipitate is still used for the classic qualitative detection and quantitative analysis of phosphorus. The crystal structure of a similar compound, with formula $H_3[PW_{12}O_{40}]$, was determined using X-ray diffraction by Keggin (1933, 1934). The names "Keggin anion" and "Keggin structure" were introduced for this polyoxotungstate and, for extension, for the whole series $[XM_{12}O_{40}]^{n-}$. There are several other structural types of polyoxoanions (Jeannin 1998). The first synthetic heteropolyniobates were obtained by Nyman et al. (2002, 2004).

The geometry, composition, and charge of these clusters are varied through synthesis parameters, and cluster properties are highly tuneable as a function of these characteristics. Recent studies of the Lindqvist ion $[H_xNb_6O_{19}]^{8-x}$ as a model compound were useful to understand aqueous reactions of geochemical interest (Black et al. 2006). Casey (2006) studied large aqueous aluminum hydroxide molecules as experimental models to determine reaction rates and pathways at a fundamental level because they expose functional groups that resemble those found on the minerals. Heteropolyanions have been employed in a range of applications that include virus-binding inorganic drugs (including the AIDs virus), homogeneous and heterogeneous catalysts, electro-optic and electrochromic materials, metal and protein binding, and as building blocks for nanostructuring of materials. The heteropolyanions of W, Mo, and V, which have

* E-mail: datencio@usp.br

found numerous applications, are formed simply by acidification of solutions of their oxoanions. Under similar conditions, these oxoanion precursors are not available for Nb, and Nb-oxo chemistry is dominated by formation of the Lindqvist ion only. However, heteropolyniobate formation is favoured in hydrothermal reactions of aqueous, alkaline precursor mixtures. The conditions of synthesis agree with the geological environment in which the new mineral was discovered. Unlike other heteropolyanions, heteropolyniobates are basic rather than acidic, which means they can survive longer and possibly even thrive in the generally basic or neutral environments of radioactive wastes and blood, respectively. Once such compounds bind with a virus, it is no longer capable of entering a cell to damage it. Heteropolyanions may also bind with radionuclides (actinides), which remove them from the mixture by phase separation for easier and safer storage (http://www.sandia.gov/news-center/news-releases/2002/mat-chem/mayday.html).

Some naturally occurring polyvanadates (as sherwoodite and pascoite) are known (Schindler et al. 2000) and an unnamed heteropolymolybdate was recently described by Kolitsch and Witzke (2005).

Menezesite has been found in the last years of the decade of 1970 by Luiz Alberto Dias Menezes Filho, but its study has begun only in May 2003. The mineral was named in honor of Menezes (born 1950), mining engineer, mineral collector, and merchant. He studied the minerals from the Jacupiranga mine (Menezes and Martins 1984) and collected the samples that were used for the first official description of several new Brazilian minerals [for instance: lanthanite-(Nd), quintinite-(2*H*), fluornatromicrolite, lindbergite, ruifrancoite, guimarãesite, and also menezesite].

The menezesite IMA number is 2005-023. Type material is deposited under the number DR458 in the Museu de Geociências, Instituto de Geociências, Universidade de São Paulo, Rua do Lago, 562, 05508-080—São Paulo, SP, Brazil.

There is no apparent relation to other mineral species.

Occurrence

The mineral occurs in the contact zone between dolomite carbonatite and "jacupirangite" (=a pyroxenite) at the Jacupiranga mine, in Cajati county, São Paulo state, Brazil (Menezes and Martins 1984). This is also the type locality for quintinite-2*H* (Chao and Gault 1997). The associated minerals are dolomite, calcite, magnetite, clinohumite, phlogopite, ancylite-(Ce), strontianite, pyrite, and tochilinite. Menezesite was formed as a vug mineral.

Habit and physical properties

Menezesite occurs as rhombododecahedra up to 1 mm (Figs. 1 and 2) isolated or in aggregates. Cleavage and twinning were not observed. The mineral is transparent and displays a vitreous luster; it is reddish brown and the streak is white. It is non-fluorescent under both short (254 nm) and long wavelength (366 nm) ultraviolet radiation. The Mohs hardness is about 4. Fracture was not determined. Density was not measured due to the paucity of material but the calculated density is 4.181 g/cm^3 (based on empirical formula). Optically the mineral is isotropic, with $n_{meas} > 1.93(1)$ (white light); n_{calc} is 2.034 using the Gladstone-Dale relationship. Menezesite exhibits weak anomalous birefringence.

Figure 1. Brownish-red rhombododecahedral crystals of menezesite, 0.5 mm, over calcite (with tiny black tochilinite inclusions).

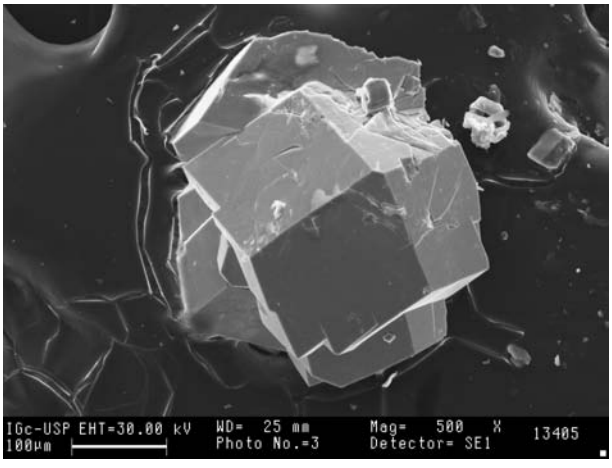

Figure 2. Secondary electron image of menezesite.

Mineral chemistry

Menezesite crystals were embedded in epoxy resin and polished. The chemical analyses (10 point analysis on different spots) were done at the Instituto de Geociências of the Universidade de São Paulo by means of a JEOL JXA-8600 electron microprobe (WDS mode, 15 kV, 20 nA, 5 µm beam diameter) and a Noran system for automation and data reduction. H_2O was inferred from the crystal-structure determination. Analytical results are represented in Table 1. No elements with $Z > 8$ other than those reported herein were indicated by EDS. The empirical formula is:

$(Ba_{1.47}K_{0.53}Ca_{0.31}Ce_{0.17}Nd_{0.10}Na_{0.06}La_{0.02})_{\Sigma 2.66}(Mg_{0.94}Mn_{0.23}Fe_{0.23}Al_{0.03})_{\Sigma 1.43}(Zr_{2.75}Ti_{0.96}Th_{0.29})_{\Sigma 4.00}[(Ba_{0.72}Th_{0.26}U_{0.02})_{\Sigma 1.00}(Nb_{9.23}Ti_{2.29}Ta_{0.36}Si_{0.12})_{\Sigma 12.00}O_{42}]\cdot 12H_2O$.

The ideal formula $Ba_2MgZr_4(BaNb_{12}O_{42})\cdot 12H_2O$ yields the following wt% oxide values: BaO = 16.40, MgO = 1.44, ZrO_2 = 17.58, Nb_2O_5 = 56.87, H_2O = 7.71, total 100.00.

Crystallographic data

Powder X-ray diffraction data (XRD) were obtained with a Siemens D5000 diffractometer equipped with a Göbel mirror

TABLE 1. Chemical composition of menezesite from Jacupiranga mine (in wt%)

Constituent	wt%	Range	Standard deviation	Probe standard
Na_2O	0.06	b.d.–0.12	0.05	Amelia albite
K_2O	0.86	0.39–1.09	0.04	K-feldspar
CaO	0.60	0.47–0.77	0.04	wollastonite
BaO	11.50	10.53–13.14	0.6	celsian
La_2O_3	0.09	b.d.–0.19	0.09	REE3
Ce_2O_3	0.94	0.74–1.29	0.1	REE3
Nd_2O_3	0.57	0.31–0.90	0.2	REE2
MgO	1.29	1.21–1.38	0.03	diopside
FeO	0.57	0.38–0.84	0.1	olivine
MnO	0.55	0.27–0.83	0.07	olivine
Al_2O_3	0.05	0.02–0.09	0.02	Areh amphibole
ZrO_2	11.58	10.86–12.53	0.4	zircon
ThO_2	4.94	4.10–5.87	0.3	ThO_2
UO_2	0.23	0.16–0.29	0.09	UO_2
TiO_2	8.90	7.86–10.38	0.4	TiO_2
Nb_2O_5	41.97	39.30–44.81	0.7	Nb
Ta_2O_5	2.71	2.06–3.24	0.4	Ta
SiO_2	0.25	0.17–0.44	0.03	wollastonite
H_2O	7.40			
Total	95.06			

Note: b.d. = below detection.

and a position-sensitive detector using Cu$K\alpha$ radiation and 40 kV and 40 μA at Instituto de Geociências of the Universidade de São Paulo (Table 2).

A single crystal was selected for intensity measurements on an Enraf-Nonius Kappa-CCD diffractometer using graphite-monochromatized Mo$K\alpha$ radiation, at the Instituto de Física de São Carlos, Universidade de São Paulo. The diffraction intensities were measured by the ω-2θ scan technique. Data collection (φ scans and ω scans with κ offsets) was made using the program COLLECT (Enraf Nonius, Delft, The Netherlands, 1997). Final cell parameters based on all reflections, integration, and scaling of the reflections intensities were performed with the HKL DENZO SCALEPACK system of programs (Otwinowski and Minor 1997). The structure was solved using direct methods and refined by full matrix least squares procedure on F^2 with SHELXL-97 (Sheldrick 1997). The crystal-structure data and characteristics of the XRD study are given in Table 3. The unit cell is cubic, and the space group is $Im\bar{3}$ (204), with $a = 13.017(1)$ Å, $V = 2206(1)$ Å^3, $Z = 2$.

Atomic coordinates, equivalent isotropic displacement parameters, occupancy, apfu, and number of electrons in each site are represented in Table 4. The ADP harmonic and anharmonic parameters of menezesite are shown in Tables 5 and 6, respectively. Selected bond lengths and angles are given in Table 7. Calculated and observed structure factors are provided in Table 8[1].

Menezesite is isostructural with the synthetic compound $Mg_7[MgW_{12}O_{42}](OH)_4{\cdot}8H_2O$ studied by Günter et al. (1990) where Mg cations occupy three different sites, named Mg1, Mg2, and Mg3. The main building unit of the structure is the $[MgW_{12}O_{42}]^{10-}$ heteropolyanion, formed by 12 face and corner sharing WO_6-octahedra, enclosing a 12-fold coordinated cavity, which is occupied by Mg (Mg3). The heteropolyanions occupy the corners and the body centered position of the unit cell and are cross-linked in three dimensions by MgO_6-octahedra to form a rigid three-dimensional lattice in two ways. In the first, Mg1 links the central polyanion to its eight neighbors in the corners

TABLE 2. X-ray powder-diffraction data for menezesite from Jacupiranga mine*

I	d_{meas} (Å)	d_{calc} (Å)	*h*	*k*	*l*
100	9.183	9.2044	0	1	1
		6.5085	0	0	2
		5.3142	1	1	2
12	4.592	4.6022	0	2	2
11	4.136	4.1163	0	1	3
		3.7577	2	2	2
		3.4789	1	2	3
16	3.256	3.2543	0	0	4
13	3.070	3.0681	0	3	3
			1	1	4
11	2.923	2.9107	0	2	4
		2.7752	2	3	3
13	2.655	2.6571	2	2	4
		2.5528	0	1	5
			1	3	4
		2.3766	1	2	5
		2.3011	0	4	4
		2.2324	0	3	5
			3	3	4
		2.1695	0	0	6
			2	4	4
		2.1116	1	1	6
			2	3	5
		2.0582	0	2	6
		2.0086	1	4	5
		1.9624	2	2	6
		1.9193	1	3	6
		1.8788	4	4	4
		1.8409	0	1	7
			0	5	5
			3	4	5
		1.8051	0	4	6
		1.7714	2	5	5
			3	3	6
			1	2	7
21	1.741	1.7395	2	4	6
		1.7092	0	3	7
9	1.650	1.6532	2	3	7
			1	5	6
		1.6271	0	0	8
		1.6023	1	4	7
			1	1	8
			4	5	5
		1.5785	0	2	8
			4	4	6
		1.5558	3	5	6
		1.5341	0	6	6
			2	2	8
11	1.5131	1.5132	1	3	8
			3	4	7
			0	5	7
		1.4932	2	6	6
		1.4739	2	5	7
6	1.4525	1.4553	0	4	8
		1.4375	0	1	9
			3	3	8
		1.4203	2	4	8
		1.4037	1	6	7
			1	2	9
			5	5	6

Note: The eight most intense reflections are in bold.
* d_{calc} from crystal structure.

[1]Deposit AM-08-002, Table 8. Deposit items are available two ways: For a paper copy contact the Business Office of the Mineralogical Society of America (see inside front cover of recent issue) for price information. For an electronic copy visit the MSA web site at http://www.minsocam.org, go to the American Mineralogist Contents, find the table of contents for the specific volume/issue wanted, and then click on the deposit link there.

of the unit cell, whereas, in the second, Mg2 links the polyanions with their six neighbors across the unit-cell faces. These latter cations complete their octahedral coordination with equatorial OH anions and water molecules in relation 1:2 to reach the electroneutrality of the compound. Günter et al. (1990) also obtained the isostructural compounds where the Mg sites are filled with Fe, Co, Mn, and Ni (Table 9).

The site "W" of Günter et al. (1990) compound is equivalent to the A site in menezesite, Mg1 to B, Mg2 to C, Mg3 to D. The sites O1, O2, and O3 are the same in the two compounds. They represent O^{2-} ions. The split O4a and O4b sites of Günter et al. (1990) compound are equal to O41 and O42, respectively, in menezesite. They are OH^--groups and H_2O-molecules in the first compound and only H_2O-molecules in menezesite. Hydroxyl groups and water molecules are distributed by electroneutrality arguments. During the procedures of structure determination two extra sites separated by ~0.5 Å were found. Trial refinements using SHELXL-97 (Sheldrick 1997) have been used with the split-atom approach for these extra sites. However, since the extra sites are very close to one another, partially empty, and occupied by different cations, poor convergence was observed during the initial refinements. It is usually observed that the closer the refined positions in a disordered structure, the higher the correlations and the more unstable the refinements when a classical split-atom approach is used in the structural model. To avoid these ambiguities, two refinements were tested: (1) a classical split-atom model considering two sites, and (2) a non-harmonic model (Kuhs 1992; Bürgi et al. 2000) based upon a development of the atomic displacement parameters (ADP) with just one site labeled as E. To perform these comparative fits the JANA2000 crystallographic computing system (Petricek et al. 2000) was used. From a statistical point of view, the model 2 is better than model 1 and also converges easier than model 1, which is probably due to lower correlations between the refined ADP and occupancy parameters. However, the main benefit of the non-harmonic model over the split-atom one for menezesite is the better match between the Ba content obtained from XRD

TABLE 3. Crystal data and experimental details

Temperature	293(2) K
Wavelength	0.71073 Å
Absorption coefficient	7.834 mm^{-1}
F(000)	2459
Crystal size	0.04 × 0.05 × 0.06 mm^3
Theta range for data collection	3.13 to 30.03°
Index ranges	$-15 \le h \le 11$, $-15 \le k \le 15$, $-15 \le l \le 15$
Reflections collected	7431
Independent reflections	310 [R_{int} = 0.1336]
Completeness to theta = 24.91°	98.4%
Refinement method	Full-matrix least-squares on F^2
Data/restraints/parameters	370/1/51
Goodness-of-fit on F^2	2.150
Final *R* indices [$I > 3\sigma(I)$]	R_1 = 0.0499, wR_2 = 0.1110
R indices (all data)	R_1 = 0.1119, wR_2 = 0.1186
Largest diff. peak and hole	1.449 and –1.152 e.$Å^{-3}$

TABLE 5. ADP harmonic parameters of menezesite

	U_{11}	U_{22}	U_{33}	U_{11}	U_{13}	U_{23}
A	0.0365(9)	0.0356(8)	0.0371(9)	0	0	–0.0016(6)
B	0.0383(6)	0.0383(6)	0.0383(6)	–0.0018(6)	–0.0018(6)	–0.0018(6)
C	0.055(10)	0.021(8)	0.061(10)	0	0	0
D	0.0319(7)	0.0319(7)	0.0319(7)	0	0	0
E	0.060(7)	0.28(2)	0.045(5)	0.025(9)	0	0
O1	0.034(4)	0.030(3)	0.027(3)	0.000(3)	–0.004(3)	0.001(3)
O2	0.030(7)	0.036(7)	0.045(8)	0	0	0
O3	0.022(4)	0.024(4)	0.037(5)	0	0.001(4)	0

The anisotropic displacement parameter exponent takes the form: $-2\pi^2[h^2a^{*2}U_{11} + ... + 2hk\ a^*\ b^*\ U_{12}]$.

TABLE 4. Atomic coordinates, equivalent isotropic displacement parameters ($Å^2 \times 10^3$), occupancy, apfu, and number of electrons for menezesite

	Mult. Wyckoff	*x/a*	*y/b*	*z/c*	U_{eq}*	atom	Occupancy	apfu‡	electrons
A	24*g*	0	0.1174(1)	0.2405(1)	36(1)	Nb	0.7683	9.22	31.50
						Ta	0.0300	0.36	2.19
						Ti	0.1917	2.30	4.22
						Σ	0.9900	11.88	37.91
B	8*c*	0.2500	0.2500	0.2500	38(1)	Zr	0.6850	2.74	27.40
						Th	0.0775	0.31	6.98
						Ti	0.2375	0.95	5.23
						Σ	1.0000	4.00	39.60
C	6*b*	0	0.5000	0	45(6)	Fe	0.0766	0.23	1.99
						Mn	0.0766	0.23	1.92
						Mg	0.3116	0.93	3.74
						Σ	0.4648	1.39	7.65
D	2*a*	0	0	0	32(1)	Ba	0.7399	0.74	41.43
						Th	0.2400	0.24	21.60
						Σ	0.9799	0.98	63.03
E	24*g*	0.391(14)	0.256(2)	0	128(8)	Ba	0.1225	1.47	6.86
						Ca	0.0258	0.31	0.52
						K	0.0442	0.53	0.84
						Σ	0.1925	2.31	8.22
O1	48*h*	0.2076(4)	0.3899(4)	0.3091(4)	30(2)	O	1.0000	24.00	8.00
O2	12*d*	0.3402(9)	0	0	37(4)	O	1.0000	6.00	8.00
O3	24*g*	0.1009(6)	0	0.1711(6)	27(3)	O	1.0000	12.00	8.00
O41	24*g*	0.3824(18)	0.3771(16)	0	33(5)†	O	0.5000	6.00	4.00
O42	24*g*	0.3581(14)	0.4175(14)	0	27(4)†	O	0.5000	6.00	4.00

* U_{eq} is defined as one third of the trace of the orthogonalized U_{ij} tensor.
† Constrained to be isotropic.
‡ For *Z* = 2.

TABLE 6. ADP anharmonic parameters of menezesite

	C_{111}	C_{112}	C_{113}	C_{122}	C_{123}	C_{133}	C_{222}	C_{223}	C_{233}	C_{333}
E	0.002(3)	–0.001(3)	0	0.036(8)	0	0.0017(15)	0.14(3)	0	0.000(3)	0

TABLE 7. Bond lengths (Å) and angles (°) for menezesite

A-O1 $^{xii, xiv}$	1.850(5)
A-O3^{iv}	1.948(8)
A-O2^{iv}	2.004(7)
A-O3^{i}	2.208(6)
A-O3	2.208(6)
B-O1	all 2.053(5)
C-O2$^{vii, ix}$	2.081(11)
C-O41$^{xvi–xix}$	2.21(2)
C-O42$^{xvi–xix}$	all 2.137(18)
D-O3$^{i–xi}$	all 2.585(8)
O1^{xiv}-A-O1^{xii}	102.0(4)
O1^{xiv}-A-O3^{iv}	98.3(2)
O1^{xii}-A-O3^{iv}	98.3(2)
O1^{xiv}-A-O2^{iv}	98.9(2)
O1^{xii}-A-O2^{iv}	98.9(2)
O1^{xii}-A-O3^{i}	92.6(3)
O3^{iv}-A-O3^{i}	82.8(4)
O2^{iv}-A-O3^{i}	75.1(3)
O1^{xiv}-A-O3	92.6(3)
O3^{iv}-A-O3	82.4(4)
O2^{iv}-A-O3	75.1(3)
O3^{i}-A-O3	72.7(3)
O1-B-O1^{xv}	90.1(2)
O1-B-O1^{viii}	90.1(2)
O1-B-O1^{xiv}	89.9(2)
O1^{xv}-B-O1^{xiv}	90.1(2)
O1^{viii}-B-O1^{xiv}	89.9(2)
O1-B-O1^{iv}	90.1(2)
O1^{xv}-B-O1^{iv}	89.9(2)
O1^{viii}-B-O1^{iv}	90.1(2)
O1^{xv}-B-O1^{xiii}	89.9(2)
O1^{viii}-B-O1^{xiii}	90.1(2)
O1^{xiv}-B-O1^{xiii}	89.9(2)
O1^{iv}-B-O1^{xiii}	90.1(2)
O2^{vii}-C-O41	all 90.0
O2^{ix}-C-O42	all 90.0
O42^{xviii}-C-O42^{xix}	62.3(10)
O42^{xviii}-C-O42^{xvi}	117.7(10)
O42^{xviii}-C-O41^{xviii}	17.7(5)
O42^{xviii}-C-O41^{xix}	80.0(8)
O41^{xviii}-C-O41^{xix}	97.7(9)
O41^{xviii}-C-O41^{xvi}	82.3(9)
O3-D-O3	all 64.26 (9)

Note: Symmetry codes as in Figure 5.

TABLE 9. Comparative data for menezesite and synthetic isostructural compounds

(all cubic, $Im\bar{3}$) compound	chemical formula	unit-cell parameter
menezesite*	$Ba_2MgZr_4(BaNb_{12}O_{42})\cdot 12H_2O$	*a* 13.017(1) Å
synthetic†	$Mg_3Mg_4(MgW_{12}O_{42})(OH)_4\cdot 8H_2O$	*a* 12.862(2) Å
synthetic†	$Mn_3Mn_4(MnW_{12}O_{42})(OH)_4\cdot 8H_2O$	*a* 13.075 Å
synthetic†	$Fe_3Fe_4(FeW_{12}O_{42})(OH)_4\cdot 8H_2O$	*a* 12.754 Å
synthetic†	$Co_3Co_4(CoW_{12}O_{42})(OH)_4\cdot 8H_2O$	*a* 12.878 Å
synthetic†	$Ni_3Ni_4(NiW_{12}O_{42})(OH)_4\cdot 8H_2O$	*a* 12.824 Å

* This work.
† Günter et al. (1990).

fit with respect to that from electron microprobe.

Menezesite structure is rich and complex: five sites are occupied by cations (A, B, C, D, E), two of them (C and E) partially emptied. A great number of cations are present, some of them with very close scattering factors. Another difficulty is that the mean electron numbers for the sites A and B are almost the same (Table 4). Consequently, it is only possible to be conclusive with respect to the geometry of the sites and to the location of the majority cations calculated from EMPA, which highlights the following ion distribution (□ = vacancies):

The following ion distribution was calculated from EMPA:

E: $(\square_{9.34}Ba_{1.47}K_{0.53}Ca_{0.31}Ce_{0.17}Nd_{0.10}Na_{0.06}La_{0.02})_{\Sigma 12.00}$

C: $(\square_{1.57}Mg_{0.94}Mn_{0.23}Fe_{0.23}Al_{0.03})_{\Sigma 3.00}$

B: $(Zr_{2.75}Ti_{0.96}Th_{0.29})_{\Sigma 4.00}$

D: $(Ba_{0.72}Th_{0.26}U_{0.02})_{\Sigma 1.00}$

A: $(Nb_{9.23}Ti_{2.29}Ta_{0.36}Si_{0.12})_{\Sigma 12.00}$

O1 to O3: O_{42}

O41 and O42: 12 H_2O

Therefore, several models were tested during successive refinements. The microprobe analysis results were used as a first approximation for cation substitutions. In all refinements, different atoms on the same site were constrained to share the same displacement parameter. The Shannon ionic radii (Shannon 1976), taking into account the suitable oxidation number of the atoms, and the geometry and environment of the sites were used as a criterion to introduce constraints in the refinement models. For instance, Ba, K, and Ca cations, due to their large ionic radii, cannot be in A, B, and C (Figs. 3, 4, and 5) and are probable in D and E. The common occurrence of the cations calculated from EMPA in other similar minerals sharing a same site was also used as approximation for the cation substitution tests. However the main approach used to reach the final cation distribution presented here was the amount of electrons that each site is able to receive keeping its maximum multiplicity. For models containing atoms with very similar scattering factors occupying the same site, some refinements gave unrealistic negative values for some atoms when the occupancy was relaxed. Therefore, the best results were obtained trying to allocate the different cations in the five possible metallic sites keeping the occupancy constrained to the total cation content calculated from EMPA. In summary, the trial models were accepted or rejected for (1) chemical reasons; (2) considering the mean electron numbers for the different metal sites; (3) paying attention to the maximum multiplicity and to the realistic values for occupancy and ADP; (4) ionic radii; (5) EMPA; (6) electronic neutrality; and (7) on the basis of the refinement results (statistical point of view). The best model was reached when all the cation populations were kept constant in agreement with the calculations by EMPA. However, when both occupation and displacement constraints were relaxed, the stoichiometric relationships remained the same for the main atoms, and similar discrepancy factors were observed. In this way, the refinement presented in Tables 3 and 4 seems to be the best model for cation distribution obtained in this X-ray diffraction experiment. The refined chemical formula and cation distribution is $(\square_{9.69}Ba_{1.47}K_{0.53}Ca_{0.31})_{\Sigma 12.00}$ $(\square_{1.61}Mg_{0.93}Mn_{0.23}Fe_{0.23})_{\Sigma 3.00}(Zr_{2.74}Ti_{0.95}Th_{0.31})_{\Sigma 4.00}[(Ba_{0.74}Th_{0.24}\square_{0.02})_{\Sigma 1.00}(Nb_{9.22}Ti_{2.30}Ta_{0.36}\square_{0.12})_{\Sigma 12.00}O_{42}]\cdot 12H_2O$ (□ = vacancies), which is in agreement with the microprobe analysis. The mean electron density in each site calculated from the cation distribution is also present in Table 4. Since sites A and B present

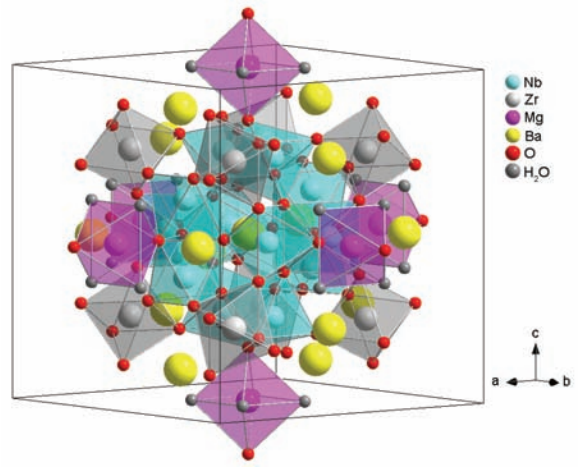

FIGURE 3. Crystal structure of menezesite. O42 not represented.

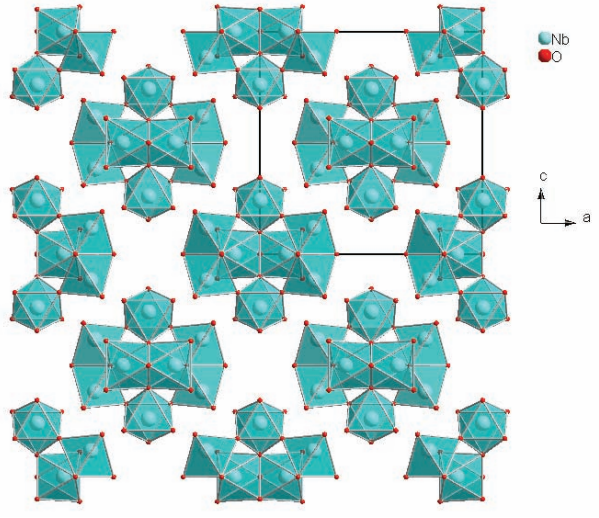

FIGURE 4. Heteropolyniobate anions in the crystal structure of menezesite.

very similar electron density, the ionic radii were necessary to propose the cation distribution of the majority cations Nb and Zr between A and B.

The main geometric parameters for these minerals are given in Table 7. Considering the cation distribution obtained by the XRD experiment (Table 4) and the Shannon ionic radii (Shannon 1976), it is possible to calculate the expected cation-oxygen bond length for the octahedrons A, B, and C: X-O = $[(X1_{Oc} * X1_{radii}) + \ldots + (Xi_{Oc} * Xi_{radii})]/\Sigma + O_{radii}$, where X is the site label, X1, X2,... Xi refer to the different cations that can occupy an individual site, O_{radii} is the oxygen ionic radii (1.25 Å), Σ is the total occupancy in each site, and the subscripts Oc and radii refer to the occupancy and ionic radii (6-coordinated, octahedral) of each atom, respectively. The calculated distances for A-O, B-O, and C-O separations are 2.02, 2.10s and 2.14 Å, respectively, which are comparable with the mean values shown in Table 7.

The site A (point symmetry *m*) has a distorted octahedral geometry with angles unevenly distributed from the ideal 90° [from 75.1(3)° to 102.0(4)°] and four independent distances, which are in the range from 1.850(5) to 2.208(6) Å. For the site B (point symmetry $\bar{3}$), which has an almost perfect octahedral geometry, the six A-O bond length are of course equivalent by symmetry [A-O = 2.053(5) Å] and angles are in the range from 89.9(1)° to 90.1(1)°. For octahedron C (point symmetry *mmm*), which is partially emptied (56% occupied), three non equivalent distances are observed. The third independent bond observed is due to the disordered sites O41 and O42 as observed by Günter et al. (1990) for $Mg_7[MgW_{12}O_{42}](OH)_4 \cdot 8H_2O$. In the D site, which is occupied by the heaviest atoms Ba and Th, the cations are coordinated to 12 oxygen ions, all of them at the same distance. The last metallic site (site E), which is partially empty (~19% occupied), is occupied by the largest cations Ba, K, and Ca. Besides its complex geometry, the ADP of the E site was treated using the non-harmonic approach as discussed above.

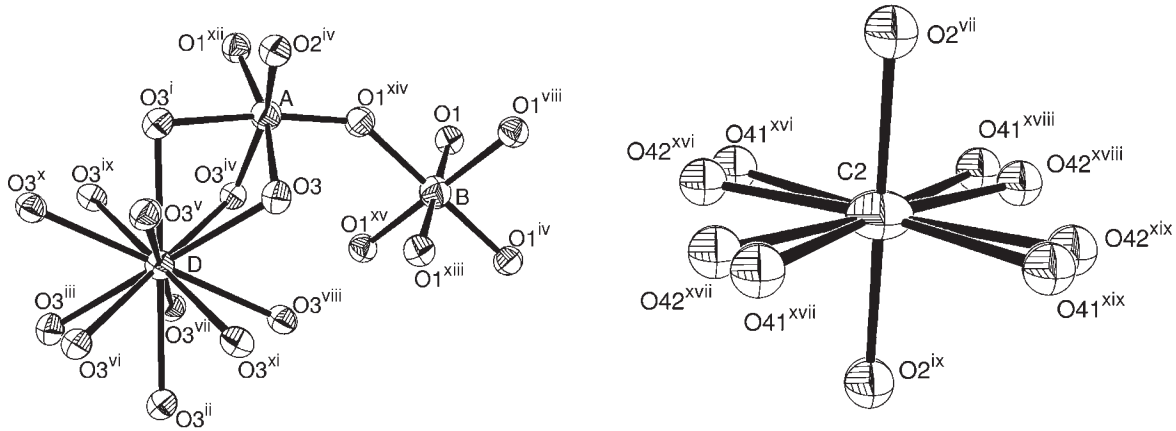

FIGURE 5. ORTEP-3 (Farrugia 1997) representation of A, B, C, and D coordination. Symmetry Codes: [i] –x, –y, z; [ii] x, –y, –z; [iii] –x, y, –z; [iv] y, z, x; [v] –y, –z, x; [vi] y, –z, –x; [vii] –y, z, –x; [viii] z, x, y; [ix] –z, x, –y; [x] –z, –x, y; [xi] z, –x, –y; [xii] y–1/2, –z+1/2, –x+1/2; [xiii] –x+1/2, –y+1/2, –z+1/2; [xiv] –y+1/2, –z+1/2, –x+1/2; [xv] –z+1/2, –x+1/2, –y+1/2; [xvi] y+1/2, z+1/2, x+1/2; [xvii] –y+1/2, –z+1/2, x+1/2; [xviii] y+1/2, –z+1/2, –x+1/2; [xix] –y+1/2, z+1/2, –x+1/2.

ACKNOWLEDGMENTS

We acknowledge FAPESP (Fundação de Amparo à Pesquisa do Estado de São Paulo) for financial support (Processes 2001/05171-0 and 2005/53741-1); the members of the Commission on New Minerals and Mineral Names of the International Mineralogical Association (CNMMN-IMA) for their helpful suggestions and comments; Geol. Rogério Kwitko Ribeiro and the Petrography Laboratory of Companhia Vale do Rio Doce, for the first EDS analyses; Isaac Jamil Sayeg and Antonio Carlos Joaquim for the EDS/WDS preliminary chemical analyses; Marcos Mansueto for assistance with the microprobe analyses; Helmut W. Schmalle and Reiner Neumann for their help with the references; Tatiana Dias Menezes for the menezesite photo (Fig. 1); the associate editor Sergey Krivovichev, Joel Brugger, and an anonymous reviewer for their construtive comments.

REFERENCES CITED

Berzelius, J.J. (1826) Beitrag zur näheren Kenntniss des Molybdäns. Annalen der Physik (Leipzig), Bd. 82; F.2/Bd.6, 369–392.

Black, J.R., Nyman, M., and Casey, W.H. (2006) Rates of oxygen exchange between the $[H_xNb_6O_{19}]^{8-x}$(aq) Lindqvist ion and aqueous solutions. Journal of American Chemical Society, 128, 14712–14720.

Bürgi, H.B., Capellia, S.C., and Birkedalb, H. (2000). Anharmonicity in anisotropic displacement parameters. Acta Crystallographica, A56, 425–435.

Casey, W.H. (2006) Large aqueous aluminum hydroxide molecules. Chemical Reviews, 106, 1–16.

Chao, G.Y. and Gault, R.A. (1997) Quintinite-2*H*, quintinite-3*T*, charmarite-2*H*, charmarite-3*T* and caresite-3*T*, a new group of carbonate minerals related to the hydrotalcite-manasseite group. Canadian Mineralogist, 35, 1541–1549.

Dale, B.W. and Pope, M.T. (1967) The heteropoly-12-niobomanganate(IV) anion. Chemical Communications, 792.

Dale, B.W., Buckley, J.M., and Pope, M.T. (1969) Heteropoly-niobates and -tantalates containing manganese(IV). Journal of Chemical Society, A, 301–304.

Farrugia, L.J. (1997) ORTEP-3 for Windows—a version of ORTEP-III with a Graphical User Interface (GUI). Journal of Applied Crystallography, 30, 565–565.

Flynn, C.M. Jr. and Stucky, G.D. (1969a) Heteropolyniobate complexes of manganese(IV) and nickel(IV). Inorganic Chemistry, 332–334.

——— (1969b) The crystal structure of sodium 12-niobomanganate (IV), $Na_{12}MnNb_{12}O_{38}{\cdot}50H_2O$. Inorganic Chemistry, 335–344.

Günter, J.R., Schmalle, H.W., and Dubler, E. (1990) Crystal structure and properties of a new magnesium heteropoly-tungstate, $Mg_7(MgW_{12}O_{42})(OH)_4(H_2O)_8$, and the isostructural compounds of manganese, iron, cobalt and nickel. Solid State Ionics, 43, 85–92.

Jeannin, Y.P. (1998) The nomenclature of polyoxometalates: How to connect a name and a structure. Chemical Review, 98, 51–76.

Keggin, J.F. (1933) Structure of the molecule of 12-phosphotungstic acid. Nature, 131, 908–909.

——— (1934) The structure and formula of 12-phosphotungstic acid. Proceedings of the Royal Society of London, A144, 75–100.

Kolitsch, U. and Witzke, T. (2005) First occurrence in nature of a mineral containing a Dawson-type heteropolyanionic cluster $[As_2Mo_{18}O_{62}]^{6-}$: Evidence from a crystal structure determination. Mitteilungen der Österreichischen Mineralogischen Gesellschaft, 151, 68.

Kuhs, W.F. (1992) Generalized atomic displacements in crystallographic structure analysis. Acta Crystallographica, A48, 80–98.

Menezes, L.A. and Martins, J.M. (1984) The Jacupiranga mine, São Paulo, Brazil. Mineralogical Record, 15, 261–270.

Nyman, M., Bonhomme, F., Alam, T.M., Rodriguez, M.A., Cherry, B.R., Krumhansl, J.L., Nenoff, T.M., and Sattler, A.M. (2002) A general synthetic procedure for heteropolyniobates. Science, 297, 996–998.

Nyman, M., Bonhomme, F., Alam, T.M., Parise, J.B., and Vaughan, G.M.B. (2004) $[SiNb_{12}O_{40}]^{16-}$ and $[GeNb_{12}O_{40}]^{16-}$: Highly charged Keggin ions with sticky surfaces. Angewandte Chemie International Edition, 43, 2787–2792.

Otwinowski, Z. and Minor, W. (1997). Processing of X-ray diffraction data collected in oscillation mode. In C.W. Carter, Jr. and R.M. Sweet, Eds., Methods in Enzimology, 276, p. 307–326. Academic Press, New York.

Petricek, V., Dusek, M., and Palatinus, L. (2000) Jana2000. The crystallographic computing system. Institute of Physics, Praha, Czech Republic.

Schindler, M., Hawthorne, F.C., and Baur, W.H. (2000) A crystal-chemical approach to the composition and occurrence of vanadium minerals. Canadian Mineralogist, 38, 1443–1456.

Shannon, R.D. (1976) Revised effective ionic radii and systematic studies of interatomic distances in halides and chalcogenides. Acta Crystallographica, A32, 751–767.

Sheldrick, G.M. (1997) SHELXL-97: Program for Crystal Structures Analysis, University of Göttingen, Göttingen, Germany.

MANUSCRIPT RECEIVED DECEMBER 11, 2006
MANUSCRIPT ACCEPTED AUGUST 18, 2007
MANUSCRIPT HANDLED BY SERGEY KRIVOVICHEV